

L. K. McMillan · R. L. Carr · C. A. Young
J. W. Astin · R. G. T. Lowe · E. J. Parker
G. B. Jameson · S. C. Finch · C. O. Miles
O. B. McManus · W. A. Schmalhofer
M. L. Garcia · G. J. Kaczorowski · M. Goetz
J. S. Tkacz · B. Scott

Molecular analysis of two cytochrome P450 monooxygenase genes required for paxilline biosynthesis in *Penicillium paxilli*, and effects of paxilline intermediates on mammalian maxi-K ion channels

Received: 8 January 2003 / Accepted: 11 June 2003 / Published online: 18 July 2003
© Springer-Verlag 2003

Abstract The gene cluster required for paxilline biosynthesis in *Penicillium paxilli* contains two cytochrome P450 monooxygenase genes, *paxP* and *paxQ*. The primary sequences of both proteins are very similar to those of proposed cytochrome P450 monooxygenases from other filamentous fungi, and contain several conserved motifs, including that for a haem-binding site.

Communicated by E. Cerdà-Olmedo

L. K. McMillan · R. L. Carr · C. A. Young · J. W. Astin
R. G. T. Lowe · B. Scott (✉)
Centre for Functional Genomics,
Institute of Molecular BioSciences, College of Sciences,
Massey University, Private Bag 11 222,
Palmerston North, New Zealand
E-mail: d.b.scott@massey.ac.nz
Tel.: +64-6-3504033
Fax: +64-6-3505688

E. J. Parker · G. B. Jameson
Centre for Structural Biology,
Institute of Fundamental Sciences, College of Sciences,
Massey University, Private Bag 11 222,
Palmerston North, New Zealand

S. C. Finch · C. O. Miles
Ruakura Agricultural Research Centre,
AgResearch, Hamilton, New Zealand

O. B. McManus · W. A. Schmalhofer · M. L. Garcia
G. J. Kaczorowski
Department of Membrane Biochemistry and Biophysics,
Merck Research Laboratories, P.O. Box 2000,
Rahway, NJ 07065, USA

M. Goetz
Department of Medicinal Chemistry,
Merck Research Laboratories, P.O. Box 2000,
Rahway, NJ 07065, USA

J. S. Tkacz
Department of Biologics Research,
Merck Research Laboratories, P.O. Box 2000,
Rahway, NJ 07065, USA

Alignment of these sequences with mammalian and bacterial P450 enzymes of known 3-D structure predicts that there is also considerable conservation at the level of secondary structure. Deletion of *paxP* and *paxQ* results in mutant strains that accumulate paspaline and 13-desoxypaxilline, respectively. These results confirm that *paxP* and *paxQ* are essential for paxilline biosynthesis and that paspaline and 13-desoxypaxilline are the most likely substrates for the corresponding enzymes. Chemical complementation of paxilline biosynthesis in *paxG* (geranygeranyl diphosphate synthase) and *paxP*, but not *paxQ*, mutants by the external addition of 13-desoxypaxilline confirms that PaxG and PaxP precede PaxQ, and are functionally part of the same biosynthetic pathway. A pathway for the biosynthesis of paxilline is proposed on the basis of these and earlier results. Electrophysiological experiments demonstrated that 13-desoxypaxilline is a weak inhibitor of mammalian maxi-K channels ($K_i = 730$ nM) compared to paxilline ($K_i = 30$ nM), indicating that the C-13 OH group of paxilline is crucial for the biological activity of this tremorgenic mycotoxin. Paspaline is essentially inactive as a channel blocker, causing only slight inhibition at concentrations up to 1 μ M.

Keywords *Penicillium paxilli* · Indole-diterpenes · Paxilline · Cytochrome P450 monooxygenases · Maxi-K channels

Introduction

Indole-diterpenes are an important group of fungal secondary metabolites, many of which are potent tremorgenic mammalian toxins (Steyn and Vleggaar 1985). They have been somewhat arbitrarily classified into six structural groups, namely the penitremes, janthitrems,

lolitrem, aflatrem, paxilline and the paspaline/paspalinine/paspalitrem (Steyn and Vleggaar 1985). To these groups can be added the more recently discovered terpendoles (Huang et al. 1995; Tomoda et al. 1995; Gatenby et al. 1999), shearinines (Belofsky et al. 1995), sulphinines (Laakso et al. 1992), nodulisporic acid (Ondeyka et al. 1997) and thiersinines (Li et al. 2002). All these compounds have a cyclic diterpene skeleton derived from four isoprene units, and an indole moiety derived from tryptophan or a tryptophan precursor (Acklin et al. 1977; de Jesus et al. 1983; Laws and Mantle 1989), but very little is known about the pathways for their biosynthesis. Biosynthetic schemes have been proposed on the basis of chemical identification of likely intermediates from the organism of interest and related filamentous fungi (Mantle and Weedon 1994; Munday-Finch et al. 1996; Gatenby et al. 1999), but until recently none of the proposed steps had been validated by biochemical or genetic studies.

We recently identified and cloned a cluster of genes from chromosome V of *Penicillium paxilli* required for the biosynthesis of the indole-diterpene paxilline (Young et al. 2001). Paxilline is a potent tremorgen (Cole et al. 1974) and a proposed intermediate in the biosynthesis of several other indole-diterpenes (Weedon and Mantle 1987; Munday-Finch et al. 1996; Gatenby et al. 1999). Although the precise boundaries of the gene cluster have still to be defined, on the basis of DNA sequence analysis the cluster is predicted to span a region of about 50 kb and to include up to 17 genes (Young et al. 2001). The identification of a geranylgeranyl diphosphate (GGPP) synthase gene (*paxG*) within this cluster, and confirmation by deletion analysis that it is necessary for paxilline biosynthesis, suggest that the synthesis of GGPP is one of the first steps in the synthesis of this indole-diterpene (Young et al. 2001). *P. paxilli*, like *Gibberella fujikuroi* (Mende et al. 1997; Tudzynski and Höltner 1998), recently renamed *Fusarium fujikuroi* (O'Donnell et al. 1998), has two GGPP synthase genes, but the second, *ggs1*, is unable to complement the *paxG* deletion, presumably because of cellular partitioning of the two enzymes (Young et al. 2001). The synthesis of paxilline is predicted to involve several oxygenation steps (Munday-Finch et al. 1996), and the presence within the cluster of genes for two FAD-dependent monooxygenases (*paxM* and *paxN*) and for two cytochrome P450 monooxygenases (*paxP* and *paxQ*) is consistent with this chemistry (Young et al. 2001).

We report here that deletion of *paxP* or *paxQ* results in mutants that are unable to synthesize paxilline. Instead they accumulate paspaline and 13-desoxypaxilline, respectively, confirming that *paxP* and *paxQ* are required for paxilline biosynthesis. In addition, we show that loss of the ability of PaxQ to hydroxylate the C-13 position of paxilline reduces by 40-fold the ability of the resulting compound, 13-desoxypaxilline, to inhibit high conductance calcium-activated (maxi-K) channels in a mammalian cell line.

Materials and methods

Fungal strains and growth conditions

Cultures of wild-type *P. paxilli* Bainier (PN2013 = ATCC 26601) and various mutant derivatives were routinely grown in PD medium (24 g/l potato dextrose; Difco, Sparks, Md., USA), PD supplemented with 0.8 M sucrose (RG medium), or 33.4 g/l Czapek-Dox (Oxoid, Basingstoke, England) supplemented with 5 g/l of yeast extract (CDYE medium), at 28°C for 7–10 days. Liquid cultures were started using an inoculum of 5×10^6 spores per 25 ml of medium, and shaken at 200 rpm for 7 days. Single spores were isolated as described previously (Young et al. 1998) and maintained on either PD agar plates or as spore suspensions in glycerol (100 ml/l) at either –20°C or –80°C.

For chemical complementation experiments cultures were grown in Medium 17 (M17), a defined medium containing per litre: 60 g mannitol, 5 g proline, 1 g K_2HPO_4 , 0.5 g $MgSO_4 \cdot 7H_2O$, 0.5 g KCl, 10 mg $FeSO_4 \cdot 7H_2O$, 10 mg $ZnSO_4 \cdot 7H_2O$, 2 mg $MnSO_4 \cdot H_2O$, 1 mg $CuSO_4 \cdot 5H_2O$, 0.8 mg $CoCl_2 \cdot 6H_2O$, buffered to pH 7.2 with 50 mM 3-(*N*-morpholino) propanesulphonic acid (MOPS). Cultures were grown at 250 rpm at 28°C. The inoculum was a 1-ml aliquot of a seed culture that had been grown for 24 h in YEPGA seed medium at 200 rpm and 28°C from spores (5×10^6 spores per 25 ml). YEPGA medium contains per litre: 10 g yeast extract, 20 g Bacto peptone, 20 g glucose, trace metals as in M17 medium (above) plus 4 g of agar, and was adjusted to pH 6.0.

Bacterial strains and plasmids

The *Escherichia coli* strain XL1 (Bullock et al. 1987) and transformants of this host were grown on LB agar plates and, where necessary, supplemented with either tetracycline (10 µg/ml) or ampicillin (100 µg/ml). Plasmids used for cloning included pUC118 (Vieira and Messing 1987), pGEM-T (Promega, Madison, Wis., USA), and pCWHygl (C. Wasmann, University of Arizona, Tucson, Ariz., USA). Plasmid pCWHygl contains the hygromycin resistance gene (*hph*) under the control of the *Aspergillus niger* glucoamylase (*glaA*) promoter and the *Aspergillus nidulans* tryptophan synthetase (*trpC*) terminator. Plasmid p56H-1 is pUC118 containing a 6.3-kb *Hin* dIII fragment cloned from λ CY56 (Young et al. 2001). Plasmid pUCHph is pUC118 containing the 2.37-kb *Xba* I fragment from pCWHygl.

Molecular biological techniques

Plasmid DNA was isolated and purified using a Concert High Purity Plasmid Miniprep System (Invitrogen, Gaithersburg, Md., USA). Genomic DNA for restriction enzyme analysis and Southern blotting was isolated using the method of Al-Samarrai and Schmid (2000). Genomic DNA for PCR was prepared from either mycelium (Yoder 1988) or from fungal spores (Ferreira and Glass 1995). In the latter method, a sterile loop of spores was transferred to a 0.5-ml Eppendorf tube, and the tube sealed and placed in a microwave oven at full power (650 W) for 5 min. TE (10 mM TRIS-HCl pH 7.5, 1 mM EDTA) buffer (30 µl) was added, the sample mixed by vortexing, and then centrifuged for 5 min at $18,000 \times g$ in a microfuge. The supernatant was collected and a 5-µl sample was used as the template for PCR. DNA fragments and PCR products were separated by agarose gel electrophoresis as previously described (Sambrook et al. 1989). DNA fragments were sequenced by the dideoxynucleotide chain-termination method (Sanger et al. 1977) using Big-Dye chemistry (Perkin-Elmer Applied Biosystems, Foster City, Calif., USA) with oligonucleotide primers synthesized by Invitrogen. Products were separated on an ABI Prism 377 sequencer (Perkin-Elmer Applied Biosystems).

PCR conditions

PCR was carried out in 25- μ l reaction volumes containing 5 μ l of DNA template (equivalent to 5 ng or less), 2.5 μ l of 10 \times reaction buffer (Roche Diagnostics, Mannheim, Germany), each primer at 200 nM, each dNTP at 50 μ M, and either 0.7 U of Expand High Fidelity polymerase (Roche) or 0.5 U of Taq DNA polymerase (Roche). For Expand Long Template PCR (Roche), reaction mixtures (50 μ l) contained 5 μ l of DNA template (1–5 ng), 5 μ l of 10 \times reaction buffer (Roche), each primer at 150 nM, each dNTP at 350 μ M, and 2.625 U of enzyme.

Genomic DNA, prepared from spores by the microwave method, was amplified in a reaction mixture (25 μ l) containing: 10 mM TRIS-HCl (pH 9.0), 50 mM KCl, 1.5 mM MgCl₂, Triton X-100 (1 ml/l), glycerol (50 ml/l), each primer at 200 nM, each dNTP at 100 μ M, and 0.7 U of Taq DNA polymerase (Roche).

The thermocycle conditions routinely used with Taq DNA polymerase and Expand High Fidelity polymerase were: one cycle for 2 min at 94°C, 30 cycles of 30 s at 94°C, 30 s at 60°C, and 1 min per kb of fragment being amplified at 72°C, and one cycle for 5 min at 72°C. When *E. coli* cells were used as the source of DNA template the initial denaturation step was increased to 5 min to allow cell lysis. The thermocycle conditions used for Long Template PCR were: one cycle for 2 min at 93°C, 10 cycles of 10 s at 93°C, 30 s at 60°C and 4 min at 68°C. This was then followed by 17 cycles starting with 10 s at 93°C, 30 s at 60°C and 3 min at 68°C, and increasing the extension time for each subsequent cycle by 20 s, and ending with one cycle for 7 min at 68°C. Reactions were carried out in a PC-960, PC-960G, or FTS-960 (Corbett Research, Mortlake, Australia) thermocycler.

Preparation of RNA, RT-PCR and rapid amplification of cDNA ends (RACE)

RNA was isolated from mycelium frozen in liquid N₂ using Trizol Reagent (Invitrogen). DNA was removed by incubating approximately 120 μ g of purified RNA with 60 U of DNase I (Roche) at 37°C for 30 min. A denatured sample (1 μ g) of this RNA was reverse transcribed using Expand Reverse Transcriptase (Roche) in the presence of either random hexamer primers (Invitrogen) or gene-specific primers. PCR was carried out with a 5- μ l aliquot of a 1/10, 1/100 or 1/1000 dilution of the cDNA as described above.

Transcription-initiation and termination sites for *paxP* and *paxQ* were determined by the RACE procedure (Frohman et al. 1988) using RNA isolated from 60-h cultures of *P. paxilli*. For 5'RACE of *paxP*, cDNA was synthesized with *cyp1*, C-tailed with terminal transferase (Roche) and amplified by nested PCR using an adapter primer, AAP, with *cyp3* for the first round, and the adapter primer AUAP with *kop1-2* for the second round. For 3'RACE of *paxP*, cDNA was synthesized with oligo-dT, then amplified by two rounds of PCR using the adapter primer UP first with *cyp8* and then with *cyp2*.

For 5'RACE of *paxQ*, cDNA was synthesized with *paxp2p5*, poly C was added with terminal transferase (Roche), and the DNA was amplified by nested PCR using the adapter primer AAP with *paxp2p5* for the first round, and the adapter primer AUAP with *paxp2p4* for the second round. For 3'RACE of *paxQ*, cDNA was synthesized with oligo-dT, then amplified by two rounds of PCR using the adapter primer UP, first with *pax34* and then with *pax60*. The specificity of the 5'- and 3'-RACE products was confirmed by a further nested PCR using the primer pairs *pax20* and *pax116*, and *pax60* and *paxp2p1*, respectively.

The PCR conditions used were as described above for cDNA synthesis. The largest PCR products from the RACE reactions were cloned into pGEM-T (Promega) and sequenced using either the M13F or M13R primer.

Construction of *paxP* and *paxQ* replacement constructs

Plasmid pLM12 (the *paxP* gene replacement vector) was constructed by sequentially ligating into pUC118, a 1269-bp *Sst* I fragment 5' of *paxP*, a 2365-bp *Xba* I fragment containing the *hph*

gene, and a 1386-bp *Sal* I fragment 3' of *paxP*. The three fragments were prepared by digesting: the PCR product amplified with primer set *kop1-3* and *kop1-2* (1295 bp) from genomic DNA, a plasmid stock of pCWHyg1, and the PCR product amplified with primer set *kop1-1* and *pax58* (1434 bp) from genomic DNA, respectively. The *kop1* primers contained mismatches relative to the genomic sequence in order to introduce *Sst* I sites at both ends of the 1295-bp fragment and a *Sal* I site at one end of the 1434-bp fragment.

Plasmid pRC3 (the *paxQ* gene replacement vector) was constructed by sequentially ligating into pUC118: a 1232-bp *Sal* I fragment 5' of *paxQ*, a 2365-bp *Xba* I fragment containing the *hph* gene, and a 1443-bp *Sst* I fragment 3' of *paxQ*. The three fragments were prepared by digesting: the PCR product amplified with the primer set *prepax1* and *prepax2* (1256 bp) from p56H-1, a plasmid stock of pCWHyg1, and the PCR product amplified with *postpax1* and *postpax2* (1460 bp) from p56H-1, respectively. The *prepax* and *postpax* primers contained mismatches to the genomic sequence, so as to introduce *Sal* I and *Sst* I sites at both ends of the 1256- and 1460-bp fragments, respectively.

P. paxilli junction fragments were amplified using Expand Hi Fidelity polymerase (Roche) as described above, except that the temperatures for annealing and extension were 55°C and 68°C, respectively. The *hph* fragment was amplified using Expand Long Template polymerase (Roche) and the primers M13F and M13R, under the PCR conditions described above. At each step in the cloning procedure the vector was digested with the appropriate restriction enzyme, treated with either shrimp or calf alkaline phosphatase (Roche) and ligated to the insert; then the mixture electroporated into XL-1 cells. The appropriate constructs were identified by PCR colony screening of the transformants. Inserted fragments were sequenced at each stage of the cloning process to confirm their sequence and orientation within the plasmid.

For transformation experiments (see below) linear products of pLM12 and pRC3, which contained the 5' gene fragment, hygromycin resistance gene (*hph*) and the 3' gene fragment, were amplified with Expand Long Template polymerase (Roche) and the primers M13F and M13R. The PCR conditions used were as described above, except that the initial extension time, for the 17 cycles, was 4 min. The PCR products were purified using a Concert Rapid PCR purification system (Invitrogen).

P. paxilli transformations

Protoplasts of PN2013 were prepared as previously described (Young et al. 1998), except that 10 mg/ml of Glucanex (Chemcolour Industries, Liestal, Switzerland) was used to digest the cell walls, and the mycelium was gently shaken (80–100 rpm) overnight at 30°C. Protoplasts were transformed with PCR-amplified linear products of pLM12 and pRC3 (see above) using the method of Vollmer and Yanofsky (1986) as modified by Itoh et al. (1994). Transformants were selected on RG medium containing hygromycin B (Roche) at a final plate concentration of 100 μ g/ml. The resulting stable transformants were maintained on PD medium with a hygromycin B concentration of 25 μ g/ml.

Molecular analysis of gene replacements

Primary screening of transformants for gene replacement events was carried out using genomic DNA prepared from spore samples (Ferreira and Glass 1995) as template and primer sets within, and external to, the gene fragment to be replaced. The PCR conditions used were the standard conditions for Taq DNA polymerase (see above), except that the annealing temperature was 55°C, and each step was for 1 min for a total of 40 cycles. A secondary round of PCR was carried out using as template genomic DNA purified either by the method of Al-Samarrai and Schmid (2000) or Byrd et al. (1990). PCR conditions used for the second round of screening were the standard conditions for Taq DNA polymerase (see above). Gene replacement mutants identified by PCR were further analysed

by Southern blotting (Southern 1975) and hybridization (Sambrook et al. 1989), using methods previously described (Young et al. 1998).

DNA sequencing

DNA was sequenced by the dideoxynucleotide chain-termination method (Sanger et al. 1977) using Big-Dye chemistry (PE Applied Biosystems) and plasmid clones as template, with oligonucleotide primers specific for pUC118 (M13F and M13R), λ GEM-11 (T7 and SP6) or *P. paxilli* sequences, synthesized by Invitrogen. Products were separated on an ABI Prism 377 sequencer (PE Applied Biosystems)

Bioinformatics

Sequence data were assembled into contigs using SEQUENCHER Version 3.1.1 (Gene Codes Corporation, Ann Arbor, Mich., USA) and analysed using the Wisconsin Package version 9.1 [Genetics Computer Group (GCG), Madison, Wis., USA]. Sequence comparisons were performed with Netscape Navigator (version 4.7) at the National Center for Biotechnology Information (NCBI) website (<http://www.ncbi.nlm.nih.gov/>) using the Brookhaven (PDB), SWISSPROT and GenBank (CDS translations), PIR and PRF databases and employing algorithms for both local (BLAST) and global (FASTA) alignments (Pearson and Lipman 1988; Altschul et al. 1990, 1997). Hydropathy values for polypeptide sequences were calculated by the methods of Kyte and Doolittle (1982) and Engelman et al. (1986) using the PEPLOT program in the Wisconsin Package (Gribskov et al. 1986). Sequences used in alignments include: *Fusarium fujikuroi* P450-1 (FfP450-1; Accession No. CAA75565) (Tudzynski and Höller 1998), *Neurospora crassa* LovA (NcLovA; CAB91316) (Schulte et al., unpublished), *F. fujikuroi* P450-4 (FfP450-4; CAA76703) (Tudzynski et al. 2001), *P. paxilli* PaxP (PpPaxP; AAK11528) (Young et al. 2001), *Coriolus versicolor* CYP512A1 (CvP450; BAB59027) (Ichinose et al. 2002), *P. paxilli* PaxQ (PpPaxQ; AAK11527) (Young et al. 2001), *Bacillus megaterium* P450 BM-3 (BmP450; 1BU7A) (Sevrioukova et al. 1999), *Oryctolagus cuniculus* P450 2C5 (Oc2C5; O4RBP4) (Pendurthi et al. 1990). For modelling purposes, the P450 2C5 enzyme as structurally characterised by Williams et al. (2000; 2C5/3LVdH) was modified in two regions: the N-terminal transmembrane region was deleted and the C-terminus of the F-helix was modified (Cosme and Johnson 2000).

Fungal P450 polypeptide sequences (Tudzynski et al. 2001; Young et al. 2001; Ichinose et al. 2002), were aligned by means of ClustalW (Higgins et al. 1994; <http://www.ebi.ac.uk/clustalw>) with the two structurally characterised P450s that shared the greatest identity, P450 BM-3 from *B. megaterium* (Sevrioukova et al. 1999) (PDB ID: 1dta) and P450 2C5 from rabbit (Williams et al. 2000) (PDB ID: 1bu7). The alignment was then modified on the basis of the structural alignment of P450 BM-3 with P450 2C5, which was made using Swiss PDB viewer (Guex et al. 2002; <http://www.expasy.ch/spdbv/>), and of the secondary structures of the fungal enzymes predicted by Psipred and threaded onto the BM-3 and 2C5 P450 structures by mGenThreader (Jones 1999a, 1999b; McGuffin et al. 2000; <http://bioinf.cs.ucl.ac.uk/psipred/>). A cross-comparison of predicted vs. observed secondary structure elements of BM-3 and 2C5 showed that Psipred tended to over-estimate the lengths of helices by one or two residues. Adopting a higher threshold (> 5 on a Psipred scale of 0–10) produced more accurate predictions of helical regions. This threshold was adopted in aligning predicted secondary structure elements of the fungal enzymes with the P450s BM-3 and 2C5. Final tuning of the structure alignments was made by assuming that the fungal P450s shared similar helix amphipathicity to that inferred from the BM-3 and 2C5 P450 structures. Except for PaxQ, Psipred predicted a single helix spanning helices C and D. However, helical propensity dropped at an LTx (x = P, R, H, Q) motif. Accordingly, helix C was terminated prior to this

motif, and helix D was begun at either the next P or one residue after a G. This led to optimal conservation of helix amphipathicity across all sequences for helices C and D. Following helix K, there is a long β loop that extends into the active site. The two-strand sheet (β 4–1 and β 4–2) is variably present in cytochrome P450 structures, and, in particular, β 4–1 is not predicted by Psipred for any of the sequences presented here.

Secondary structure predictions by Psipred were confirmed by Prosite (Bairoch et al. 1997) and GorIV (Garnier et al. 1996). Relative to the ClustalW sequence alignment, incorporation of secondary-structure information produces a substantially different sequence alignment for the A helix. Comparison of observed structures of BM-3 and 2C5 further emphasizes that sequence identity should not be expected always to correlate with structural identity—this is particularly apparent in the alignment of the C-terminal β loop.

Indole-diterpene analysis

Mycelial pellets from a 25-ml culture of *P. paxilli* grown for 7 days in CDYE were washed with Milli-Q water (Millipore, Bedford, Mass., USA), snap frozen and freeze dried. Indole-diterpenes were extracted by homogenising the pellets in 15 ml of a 2:1 mixture of chloroform-methanol. After mixing for 1 h, the samples were centrifuged at 18,000 \times g in a bench centrifuge for 10 min to pellet the insoluble material. For analysis by thin layer chromatography (TLC) 1.5 ml of the supernatant was dried down under a stream of N₂ and resuspended in 50 μ l of chloroform-methanol (2:1). Aliquots (5 μ l) of this material were fractionated on SIL G (Macherey-Nagel, Düren, Germany) TLC plates using a 9:1 chloroform-acetone mixture. Indole-diterpenes were identified either by their UV (254 nm) fluorescence or by their colour after spraying the plates with alcoholic Ehrlich's reagent (2 g/l *p*-dimethylamino-benzaldehyde in 120 ml/l HCl and 500 ml/l ethanol] and heating to 100°C for 5 min.

For analytical HPLC a 2.0-ml sample was evaporated under a stream of N₂, then redissolved in 1.0 ml of either dichloromethane (DCM) for normal phase or methanol for reverse phase. Samples (10 μ l) were analysed on either a Waters 600 (normal phase; Waters Corporation, Milford, Mass., USA) or Dionex Summit (reverse phase; Dionex Corporation, Sunnyvale, Calif., USA) HPLC using Zorbax (Rockland Technologies, Nuenen, The Netherlands) silica gel (4.6 \times 250 mm, 5 μ m bead diameter) or Luna (Phenomenex, Torrance, Calif., USA) C18 (4.6 \times 250 mm, 5 μ m) columns, respectively. As mobile phases DCM:acetonitrile (95:5 or 80:20) containing methanol (4 ml/l) and methanol-water (85:15) were used, at flow rates of run at 1.8 ml/min and 1.5 ml/min, respectively. All samples and solvents were filtered through 0.45 μ m nylon filters (Millipore) before analysis. Eluted products were analysed by UV spectrophotometry at either 230 or 280 nm and compared with the elution times of ergosterol, 13-desoxypaxilline, paspaline and paxilline standards. Samples were quantified with respect to known concentrations of the same standards. The sensitivity of detection was approximately 50 to 100 ng.

For preparative HPLC of extracts from LMQ-226, samples (900 μ l) were separated on a silica gel (Ranin Instruments, Emeryville, Calif., USA) column (21 \times 250 mm, 5 μ m) using DCM:acetonitrile (70:30) plus methanol (4 ml/l) as the mobile phase (at 10 ml/min). The fraction containing 13-desoxypaxilline, which elutes at 10 min, was collected manually and concentrated on a rotary evaporator. Subsequent fractions were pooled, the mixture resuspended in acetone, and the purity of the sample confirmed by analytical normal-phase (DCM-acetonitrile; 95:5 containing 4 ml/l methanol) HPLC. A single UV (230 nm) absorbing peak with a retention time of 5.4 min, corresponding to that of authentic 13-desoxypaxilline, was observed. Addition of 13-desoxypaxilline to samples confirmed that the purified compound co-eluted with authentic 13-desoxypaxilline. While 13-desoxypaxilline was the only indole-diterpene detected, other non-UV absorbing compounds may still be present in this sample. A total of 3 mg of 13-desoxypaxilline was obtained from 33 ml of fungal culture.

Chemical complementation of *pax* mutants

P. paxilli mutants were grown for 4 days in M17 medium in the presence of hygromycin (50 mg/l), the mycelium was washed in 1 mM MOPS (pH 7), and a 1-g (wet weight) sample was resuspended in 10 ml of 20 mM MOPS (pH 7) containing mannitol (6 g/l) and hygromycin (50 g/l). A 100- μ l aliquot of the 13-desoxypaxilline stock (1 g/l in acetone) was then added to the culture. After 24 h growth, a second 100- μ l aliquot of 13-desoxypaxilline was added, and the culture was incubated for a further 24 h. The mycelia were harvested, freeze dried (approximately 0.1 g dry weight) and extracted with 4 ml of chloroform:methanol (2:1). The dried extract was resuspended in 1 ml of DCM and analysed for indole-diterpenes by analytical HPLC as described above.

Construction of a stable cell line expressing maxi-K channels

HEK293 cells were stably transfected with the genes encoding alpha and beta1 subunits of the maxi-K channel from human. HEK293 cells were plated in 100 mm tissue culture dishes. Fifteen hours after plating, the cells were transfected with the genes for maxi-K alpha and beta1 subunits using FuGENE 6 (Roche). The gene for the alpha subunit was inserted in the pCIneo vector (Promega; Hanner et al. 1997), for selection with geneticin, and the beta1 subunit gene (Uebele et al. 2000) was cloned in the pIRESpuro vector (Clontech, Palo Alto, Calif.), for selection with puromycin. The maximum antibiotic concentration for selection was previously determined to be 50 mg/l for geneticin, and 0.75 mg/l for puromycin. Transfected cells were grown under this level of selection until distinct single colonies could be isolated. Groups of five colonies were collected and transferred to 6-well tissue-culture plates, and grown under selection until confluent monolayers were established. Cells were then tested for levels of maxi-K channel expression by monitoring binding of the selective maxi-K channel blocker [¹²⁵I]iberiotoxin-D19Y/Y36F (IbTX-D19Y/Y36F) (Giangiacomo et al. 2000). Those cells that gave the largest binding signal were diluted to about five cells per ml, and 200- μ l portions were plated into single wells of a 96-well tissue culture plate. Cells were grown under selection, and expanded, until a confluent T-25 flask of each single colony was obtained. Cells were tested again for maxi-K channel expression, and the cell line yielding the best results was expanded and frozen for further studies.

Electrophysiological methods

Patch clamp recordings were made on excised inside-out patches using standard methods (Hamill et al. 1981). Membrane patches

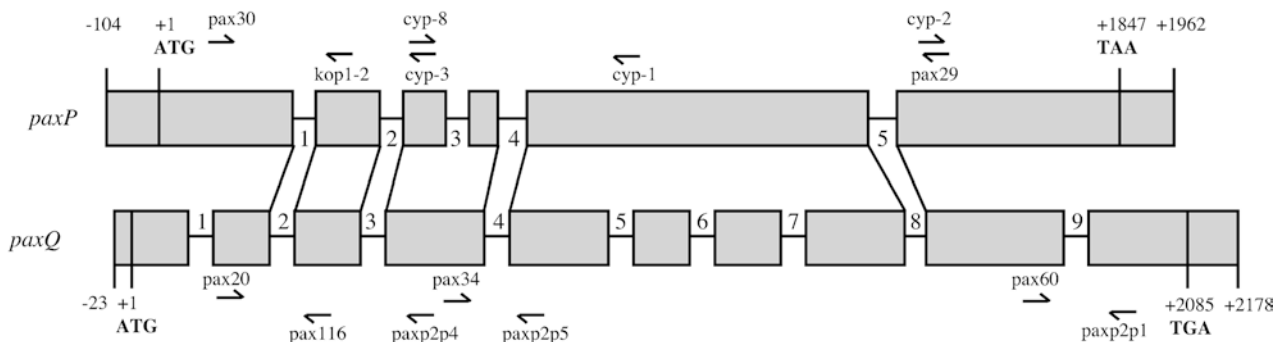
were excised from HEK293 cells stably expressing the alpha and beta1 subunits of maxi-K channel, so that the intracellular side of the channels was in direct contact with the bath solution. Membrane currents were recorded with an EPC-9 amplifier (HEKA Instruments, Lambrecht, Germany) and data acquisition was controlled with PULSE software (HEKA Instruments). Data analysis and figure preparation was done using PULSEFIT (HEKA Instruments) and IGOR Pro (Wavemetrics, Lake Oswego, Ore., USA) software. Pipettes were pulled from Garner 7052 glass (Garner Glass, Claremont, Calif., USA) and typically had resistances of 1–3 m Ω when filled with experimental solutions. Bath and pipette solutions contained 150 mM KCl, 10 mM HEPES, 2 mM MgCl₂ and 0.1 mM CaCl₂, and the pH was adjusted to 7.2 with KOH. Compounds were dissolved in DMSO at 10–20 mM and stored frozen at –20°C. Prior to use the compounds were thawed and diluted in the experimental solution, so that the final DMSO concentration was always less than 1 g/l (a concentration that had no effect on channel function in our experiments). The bath (volume of about 0.1 ml) was constantly perfused at a rate of about 1 ml/min. If current magnitude was stable for at least 10 min, control bath solution was switched to an experimental solution allowing drug application to the cytoplasmic side of the channels. The membrane potential was held at –80 mV and voltage ramps (–100 to +50 or +100 over 1 s) were applied every 15 s. The slope conductance was measured over a linear range (0 to +20 mV) where channel open probability was near maximal, giving an estimate of the number of channels available for opening. The fraction of unblocked (FUB) channels in different conditions was calculated and fitted to a Hill equation of the form $FUB = 1/(1 + K_i/\text{concentration}) - 1$. Experiments were done at room temperature (22–25°C).

Results

Molecular analysis of *paxP* and *paxQ*

Sequence analysis of *paxP* predicted that it contains five introns (Fig. 1). This was confirmed experimentally by sequencing a cDNA product amplified with the primer pair *pax30* and *pax29* using mRNA isolated from 60-h cultures of *P. paxilli*. The transcription start and stop sites for *paxP* were determined by sequencing 5' and 3' RACE products. These results indicated that the transcription start lies 104 bp upstream of the ATG and the transcription stop is located 113 bp from the TAA. Sequences similar to the consensus RNA polymerase binding and polyadenylation motifs (TATAA and AATAAA) are found immediately upstream of the proposed transcription initiation and termination points. These data indicate that *paxP* produces a

Fig. 1 Structure of the genes *paxP* and *paxQ*. Schematic diagrams of *paxP* and *paxQ* showing the positions of exons, introns, transcriptional start and stop sites and primers used for cDNA synthesis and analysis



primary transcript of approximately 2066 nt that encodes a polypeptide (PaxP) of 515 amino acids with a predicted molecular weight of 58.8 kDa.

In contrast, *paxQ* has nine introns (Fig. 1). Introns 2–9 were confirmed by sequence analysis of a cDNA product amplified with the primer set *pax20* and *paxp2p1*, and intron 1 by analysis of the sequence of the 5' RACE product. All introns have conserved 5' GT and 3' AG splice junctions, with the exception of the 3' splice junction of intron 1, which is TG. A 3' splice recognition sequence of TG rather than the consensus AG is unusual (Mount 1982). While variations in the AG consensus are found, these changes usually reduce the efficiency of step two of the splicing reaction and lead to reduced levels of steady-state mRNA (Parker and Siliciano 1993; Deirdre et al. 1995). Sometimes compensatory mutations are found in the 5' GT splice site (Deirdre et al. 1995), but this does not appear to be the case for intron 1 of *paxQ*. The positions of introns 2, 3, 4 and 8 in *paxQ* correspond to those of introns 1, 2, 4 and 5 in *paxP* (Fig. 1). The transcription start and stop sites for *paxQ* were determined by sequencing 5' and 3' RACE products. These results indicate that *paxQ* transcription initiates just 23 bp upstream of the translational start site. Although the 5' untranslated region is therefore very short, its size is within the range found for genes of filamentous fungi (Gurr et al. 1987; Unkles 1992). No TATAA box motifs are present within 300 bp upstream of this proposed transcription start-site. In addition, no obvious polyadenylation signal sequence (AATAAA) is found in the 3' untranslated region of this gene. The RACE results indicate that *paxQ* produces a primary transcript of approximately 2201 nt that encodes a polypeptide (PaxQ) of 512 amino acids with a predicted molecular weight of 58.2 kDa.

Structural analysis of PaxP and PaxQ

PaxP and PaxQ are most similar in sequence to other fungal cytochrome P450 enzymes, as revealed by analysis with BlastP (Altschul et al. 1997) and FASTA (Pearson and Lipman 1988). In particular, PaxP (PaxQ) shows over its full length of ~490 residues ~35% (27%) identity to P450-1 and P450-4, which form part of the gibberellin biosynthetic pathway in *Fusarium fujikuroi* (Tudzynski and Höltner 1998; Tudzynski et al. 2001), and ~34% (31%) identity to CvP450, a cytochrome P450 of unknown function from *Coriolus versicolor* (Ichinose et al. 2002). The proteins show a similar degree of identity to LovA from *Neurospora crassa* (Schulte et al., unpublished). PaxP and PaxQ share 27% identity. Analysis of the hydrophobicity of the two proteins (Kyte and Doolittle 1982; Engelman et al. 1986) predicts that both contain a single transmembrane helical domain at the N-terminus.

A comparison of fungal P450 polypeptide sequences with those of the structurally characterised bacterial BM-3 and mammalian 2C5 cytochrome P450s using

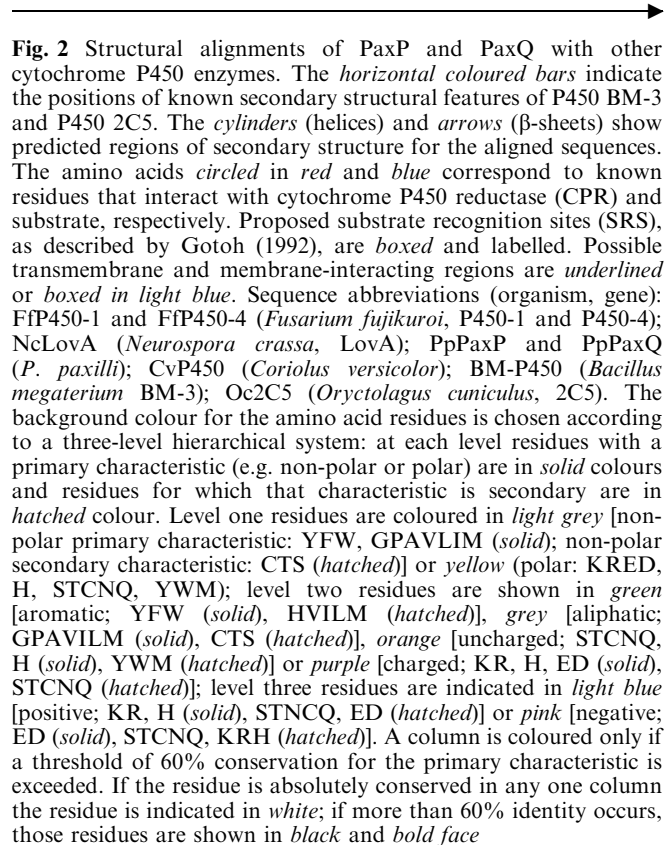


Fig. 2 Structural alignments of PaxP and PaxQ with other cytochrome P450 enzymes. The horizontal coloured bars indicate the positions of known secondary structural features of P450 BM-3 and P450 2C5. The cylinders (helices) and arrows (β -sheets) show predicted regions of secondary structure for the aligned sequences. The amino acids circled in red and blue correspond to known residues that interact with cytochrome P450 reductase (CPR) and substrate, respectively. Proposed substrate recognition sites (SRS), as described by Gotoh (1992), are boxed and labelled. Possible transmembrane and membrane-interacting regions are underlined or boxed in light blue. Sequence abbreviations (organism, gene): FfP450-1 and FfP450-4 (*Fusarium fujikuroi*, P450-1 and P450-4); NcLovA (*Neurospora crassa*, LovA); PpPaxP and PpPaxQ (*P. paxilli*); CvP450 (*Coriolus versicolor*); BM-P450 (*Bacillus megaterium* BM-3); Oc2C5 (*Oryctolagus cuniculus*, 2C5). The background colour for the amino acid residues is chosen according to a three-level hierarchical system: at each level residues with a primary characteristic (e.g. non-polar or polar) are in solid colours and residues for which that characteristic is secondary are in hatched colour. Level one residues are coloured in light grey [non-polar primary characteristic: YFW, GPAVLIM (solid); non-polar secondary characteristic: CTS (hatched)] or yellow (polar: KRED, H, STCNQ, YWM); level two residues are shown in green [aromatic: YFW (solid), HVILM (hatched)], grey [aliphatic: GPAVILM (solid), CTS (hatched)], orange [uncharged; STCNQ, H (solid), YWM (hatched)] or purple [charged; KR, H, ED (solid), STCNQ (hatched)]; level three residues are indicated in light blue [positive; KR, H (solid), STCNQ, ED (hatched)] or pink [negative; ED (solid), STCNQ, KRH (hatched)]. A column is coloured only if a threshold of 60% conservation for the primary characteristic is exceeded. If the residue is absolutely conserved in any one column the residue is indicated in white; if more than 60% identity occurs, those residues are shown in black and bold face

ClustalW (Higgins et al. 1994) and mGenThreader (Jones 1999a, 1999b; McGuffin et al. 2000) gave sequence identities in the range 12–16%. BM-3 (*Bacillus megaterium*; PDB ID: 1dta; Sevrioukova et al. 1999) and 2C5 (rabbit, PDB ID 1bu7; Williams et al. 2000) share only 16% sequence identity and superimpose with an RMS value of 1.56 Å. The structural alignment of these P450s is shown in Fig. 2. PaxP and PaxQ, and the other fungal enzymes, are predicted to share the predominantly helical secondary structure seen in other structurally characterised cytochrome P450s (Degtyarenko 1995). Indeed, all secondary structure elements common to BM-3 and 2C5 were predicted for the fungal enzymes, notwithstanding the very low sequence identity especially in the N-terminal regions. More significantly, the amphipathicity of helical elements, in particular, is remarkably well conserved across all sequences shown in Fig. 2.

The most highly conserved structural elements of P450 enzymes include a four-helix bundle consisting of helices D, I, L and E, helices J and K, β -sheets 1 and 2, the haem-binding domain, and the “meander”, which precedes the haem-binding domain (Graham-Lorence and Peterson 1996). There are 13 absolutely conserved amino-acid residues, which include phenylalanine, glycine, cysteine and glycine in the haem-binding domain, and the glutamate and arginine in the K helix. The haem-binding region contains the essential cysteine residue required to form the fifth ligand to the haem iron. With respect to the F(G/S)xGx(H/R)xCxGxx(I/L/F)A



consensus sequence (Graham-Lorence and Peterson 1996), there are conservative substitutions at the sixth position in PaxP and at the thirteenth position in PaxQ. The K helix stabilises the core of the enzyme and contains the absolutely conserved ExxR motif, which forms a salt bridge and faces into the “meander” region of the

enzyme. Helix I is the longest helix in P450 enzymes, and runs through the centre of the structure. The threonine-serine-rich motif, E(T/S)(T/S)(S/T/A) motif is preserved in PaxP and PaxQ, although the glutamate is replaced by histidine. The L helix, which lies in close proximity to the haem grove, is the most conserved helix in the

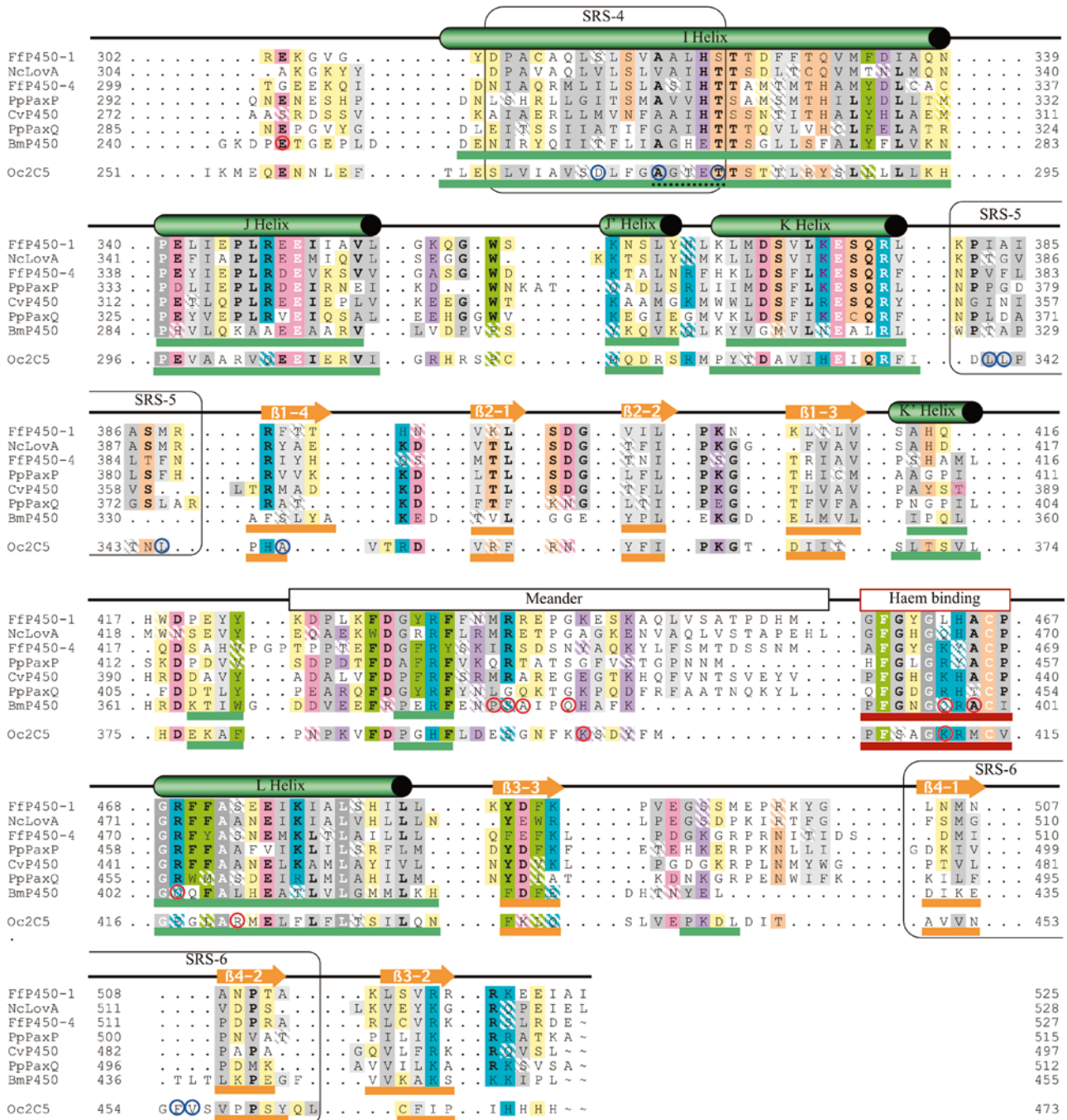


Fig. 2 (Contd.)

alignment (Sevrioukova et al. 1999; Williams et al. 2000). The J helix contains two residues that are subject to strong functional constraints. The proline positioned at the beginning of the J helix is conserved in all the sequences aligned. A glutamate is also observed in all J helix sequences. It appears to interact with the backbone exposed at the N-terminus of the K helix. In the otherwise weakly conserved N-terminal region, a conserved glutamate residue that is found in helix B appears to hydrogen bond with the backbone of the beta 2-1 to 2-2 turn in the C-terminal region.

Deletion of *paxP* and *paxQ*

To confirm that *paxP* and *paxQ* encode enzymes involved in paxilline biosynthesis, replacement constructs, pLM12 and pRC3, were prepared and linear forms of these were recombined into the genome of the wild-type strain (Fig. 3). Out of a total of 200 primary transformants that carried the *paxP* construct, 75 (38%) were unstable. The remaining 93 were screened by spore PCR (Ferreira and Glass 1995) for a replacement event using primer sets that amplify upstream (*pax36* and *pax129:235* bp), internal (*cyp1* and *cyp8:532* bp) and downstream (*pax127* and *pax27:767* bp) regions of *paxP*.

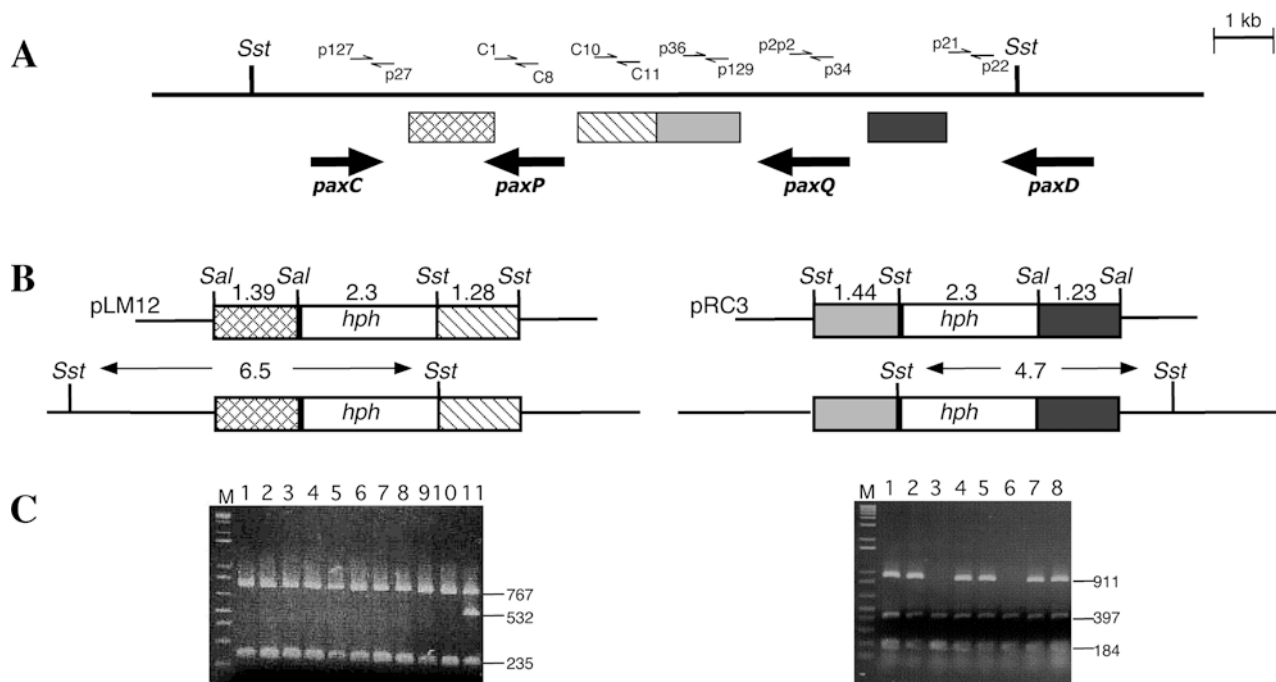


Fig. 3A–C Deletion of *paxP* and *paxQ*. **A** Physical map of the *paxP* and *paxQ* regions of the paxilline biosynthesis gene cluster (Young et al. 2001). Primers used for screening gene replacements are shown above the map and the regions exchanged (shaded) below the map. **B** Physical maps of *paxP* and *paxQ* replacement constructs (upper line) and products of the recombination (lower line). **C** PCR products generated using primer sets (see text) that amplify both internal and flanking regions of the *paxP* (left) and *paxQ* (right) replacements, respectively. Lanes 1–11 on the left were loaded with PCR products obtained from the *paxP* mutants LMP-1, -2, -11, -14, -16, -18, -26, -48, -57, -61 and wild-type, respectively. Lanes 1–7 on the right were loaded with PCR products obtained from the *paxQ* mutants LMQ-206, -208, -212, -214, -217, -226, -228 and wild-type, respectively. Fragment sizes are given in bp. An aliquot of the BRL 1 Kb⁺ ladder was loaded in lane M

Ten transformants were identified as gene replacements (results not shown). This result was confirmed by re-screening with the same set of primers but using purified genomic DNA (Al-Samarrai and Schmid 2000) as template (Fig. 3C). All 10 mutants lacked the 532-bp internal fragment (Fig. 3C; lanes 1–10) found in the wild type (lane 11), but retained the flanking sequences indicative of a double cross-over. Southern analysis of *Sst* I genomic digests probed with an internal 974-bp fragment of *paxP*, amplified with *pax29* and *cyp8* (see Fig. 1), confirmed that all mutants lacked this region, whereas a 12.7-kb fragment (see Fig. 3A) hybridized in the wild-type sample (results not shown). Probing the same blot with a 2.5-kb *hph* fragment, amplified from pUCHph, showed that three of the mutants, LMP-1, LMP-48 and LMP-57, were ‘perfect’ replacements, each with a single hybridising 6.5-kb fragment (Fig. 4A). The other seven were a mixture of single-site/multicopy integrations (LMP-11, LMP-14, LMP-16, LMP-18, LMP-26), with 6.5-kb and 3.7-kb (multi-copy) hybridising bands, and multi-site/multi-copy (LMP-2, LMP-61) integrations, with additional hybridising bands (Fig. 4A)

Out of a total of 60 primary transformants obtained with the *paxQ* construct, 23 (38%) were unstable. The remaining 37 were screened by spore PCR (Ferreira and Glass 1995) for a replacement event using a primer set (*paxp2p2* and *pax34*) designed to amplify within *paxQ* (Fig. 3A). Seven lacked the 911-bp internal fragment (results not shown). Genomic DNA was purified (Al-Samarrai and Schmid 2000) from these and re-screened by PCR for replacements using primer sets that amplify upstream of (*pax21* and *pax22*:184 bp), internal to (*paxp2p2* and *pax34*:911 bp) and downstream (*cyp10* and *cyp11*:397 bp) of *paxQ* (Fig. 3A). Two of the transformants, LMQ-212 and LMQ-226, were confirmed to have gene replacements (Fig. 3C; lanes 3 and 6). Southern analysis of *Sst* I genomic digests probed with an internal 1907-bp fragment, amplified with *pax20* and *paxp2p1* (see Fig. 1), confirmed that both mutants lacked this region, whereas a 12.7-kb fragment (see Fig. 3A) hybridized in the wild-type sample (results not shown). Probing the same blot with a 2.5-kb *hph* fragment showed that LMQ-226 is a ‘perfect’ replacement containing a single 4.7-kb hybridising band (Fig. 4B). LMQ-212 has additional copies of the construct integrated in one of the junction fragments (3.5-kb multi-copy band) and at an ectopic site (6.9-kb band) (Fig. 4B).

Chemical phenotype of *paxP* and *paxQ* deletion mutants

To determine the chemical phenotype of the *paxP* and *paxQ* mutants, methanol/chloroform extracts were prepared from 7-day-old cultures grown in CDYE, and indole-diterpenes were analysed by TLC. Paxilline was

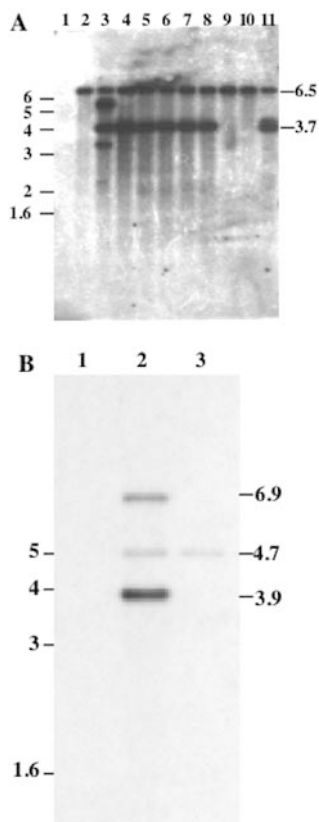


Fig. 4A, B Southern analysis of *paxP* and *paxQ* deletions. Southern blots of *Sst* I digests of *P. paxilli* wild-type and mutant genomic DNAs (1 μ g/lane) probed with a 32 P-labelled *hph* fragment amplified from pUChph using M13F and M13R primers. **A** Lanes 1–11: wild-type, LMP-1, -2, -11, -14, -16, -18, -26, -48, -57, and -61. **B** Lanes 1–3: wild-type, LMQ-212 and -226. Fragment sizes for the 1-kb ladder (*left*) and hybridising bands (*right*) are shown in kb

absent ($R_f=0.41$) from both sets of mutant extracts, and instead new green-staining compounds with R_f values of 0.61 and 0.65, identical to the R_f s of paspaline and 13-desoxypaxilline standards, were present in the extracts of *paxP* and *paxQ* mutants, respectively (results not shown). To confirm the identity of the new products that accumulate in these mutants, extracts were analysed by normal- and reverse-phase HPLC. Reverse-phase analysis of extracts from the *paxP* deletion mutant LMP-1 (Fig. 5B) and the wild-type strain (Fig. 5A) showed that the mutant fails to synthesize detectable levels of paxilline, which has a retention time of 5.5 min. Instead, this mutant accumulates a new product which has the same retention time (21 min) as authentic paspaline and co-elutes with it (results not shown). When extracts of mutant LMP-1 were analysed by normal-phase HPLC the product that accumulated had the same retention time (5.8 min) as paspaline and co-eluted with it (results not shown). Analysis of the mutants LMP-11, LMP-14 and LMP-57 confirmed that they also accumulated paspaline.

Reverse-phase HPLC analysis of extracts of the *paxQ* deletion mutant, LMQ-226 (Fig. 5D), and the wild type

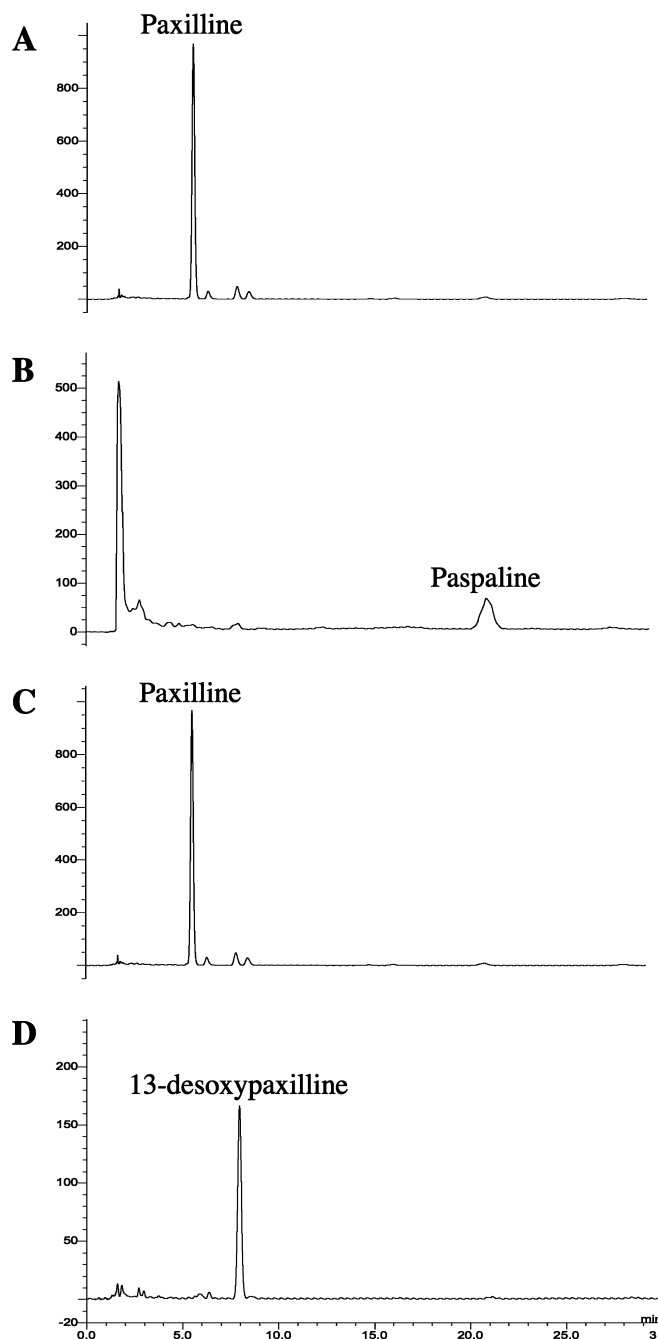


Fig. 5A–D HPLC analysis of indole-diterpenes in extracts of wild-type *P. paxilli*, and *paxP* and *paxQ* mutants. Mycelia were harvested after 7 days of growth and analysed for indole-diterpenes by reverse phase HPLC. **A** Wild type. **B** *paxP* mutant LMP-1. **C** Wild type. **D** *paxQ* mutant LMQ-226. The y-axis is calibrated in milliabsorbance units at 230 nm (A_{230nm}) and the retention time in min is shown on the x-axis

(Fig. 5C), showed that this mutant lacks detectable levels of paxilline. Instead it accumulates an indole-diterpene with the same retention time (8 min) as authentic 13-desoxypaxilline and co-elutes with it (results not shown). When extracts of mutant LMQ-226 were analysed by normal-phase HPLC the product that accumulated had the same retention time (5.4 min) as

13-desoxypaxilline and co-eluted with it (results not shown). Analysis of mutant LMQ-212 confirmed that it also accumulates 13-desoxypaxilline.

Addition of 13-desoxypaxilline to the culture medium restores paxilline biosynthesis in *paxG* and *paxP* mutants, but not in *paxQ*

To confirm that 13-desoxypaxilline is indeed an intermediate in the biosynthesis of paxilline, and that mutants lacking enzymes for proposed earlier steps in the pathway (Munday-Finch et al. 1996) are still capable of paxilline biosynthesis, a chemical complementation experiment was carried out. Addition of 13-desoxypaxilline to cultures of LMP-1 and a previously isolated *paxG* mutant, LMG-23 (Young et al. 2001), resulted in the synthesis of an indole-diterpene that co-elutes (at 4 min) with paxilline (Fig. 6B and C). As expected, LMQ-226 was unable to convert 13-desoxypaxilline into paxilline (Fig. 6A). Under these HPLC conditions paspaline, ergosterol and 13-desoxypaxilline co-elute at 3.0 min (Fig. 6A–C). These results were confirmed by analysing the same samples by reverse-phase HPLC (results not shown).

Ion channel blocking activity of paxilline, 13-desoxypaxilline and paspaline

The high levels of paspaline and 13-desoxypaxilline that accumulate in the *paxP* (LMP-1) and *paxQ* (LMQ-226) mutants, compared to the wild-type culture, makes them a convenient biological source of material for purifying these compounds to analyse their biological properties. Using these mutants, both compounds were purified, and their effects on maxi-K channel function were examined using electrophysiological methods. Patch clamp recording methods (Hamill et al. 1981) were used to isolate, and record currents from, small patches of plasma membrane from cells that constitutively express alpha and beta1 subunits of the maxi-K channel. The patches were excised in the inside-out configuration, so that the intracellular side of the membrane was in contact with the bath solution. Figure 7A shows a recording from a patch containing more than 500 maxi-K channels, where the membrane potential is ramped from -100 mV to $+50$ mV over 1 s. In the control, with $10 \mu\text{M}$ internal calcium, a large voltage-dependent current, activated at voltages more positive than -100 mV, was maximally activated at voltages greater than 0 mV, and reversed polarity at 0 mV, as required for a potassium channel in symmetrical KCl. This current was eliminated after reducing internal calcium to less than 10 nM by perfusing with bath solution containing 1 mM EGTA and no added calcium (Fig. 7A and B), demonstrating that all the current is calcium sensitive. The range of negative slope conductance seen between -100 mV and -40 mV reflects an increase in the open probability for the maxi-K

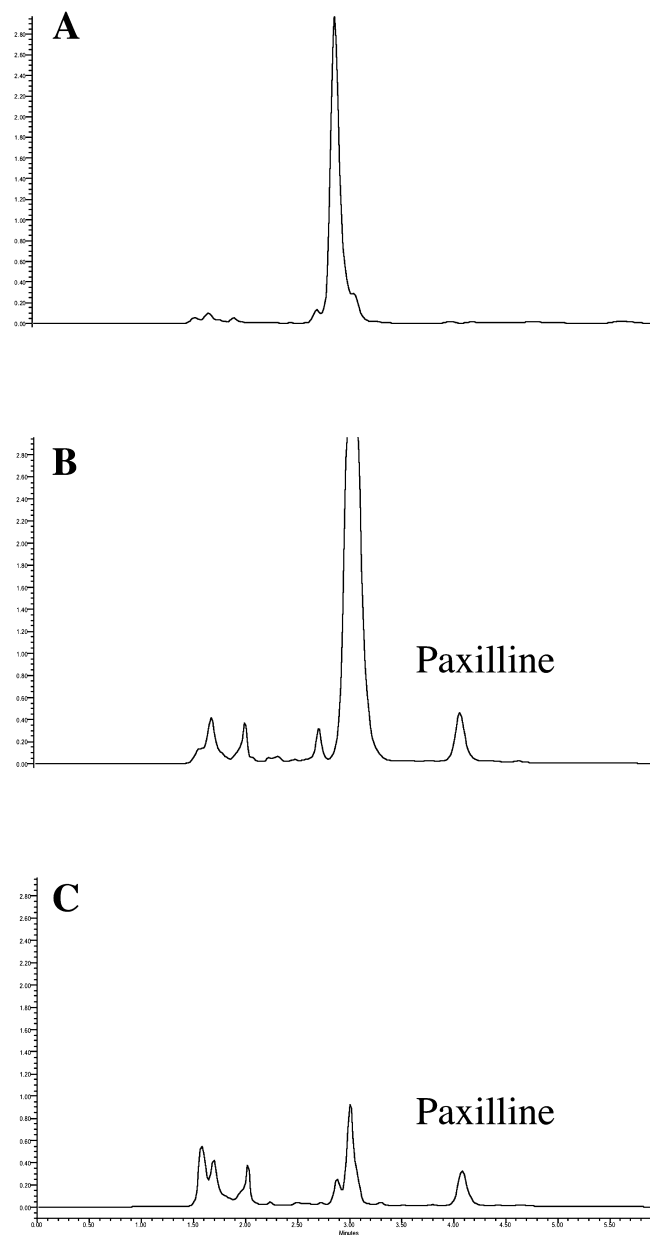


Fig. 6A–C Complementation of paxilline biosynthesis in *paxG* and *paxP* mutants by addition of 13-desoxypaxilline to the culture medium. Mycelia of *paxG*, *paxP* and *paxQ* mutants were grown in the presence ($200 \mu\text{g}$ per 10-ml culture) of 13-desoxypaxilline, and extracts were analysed for paxilline by normal-phase HPLC. **A** *paxQ* mutant LMQ-226. **B** *paxP* mutant LMP-1. **C** *paxG* mutant LMG-23. The y-axis is calibrated in absorbance units at 230 nm ($A_{230\text{nm}}$) and the retention time in min is shown on the x-axis

channel from mostly closed at -100 mV to fully open at 0 mV. The shape of the current-voltage relation recorded during the voltage ramps is a product of a linear component passing through the axis center that describes conductance of open channels and an increasing sigmoid function with a midpoint at approximately -40 mV that results from the voltage-dependence of channel opening. These characteristic properties of voltage- and calcium-dependent gating are consistent with previous reports of

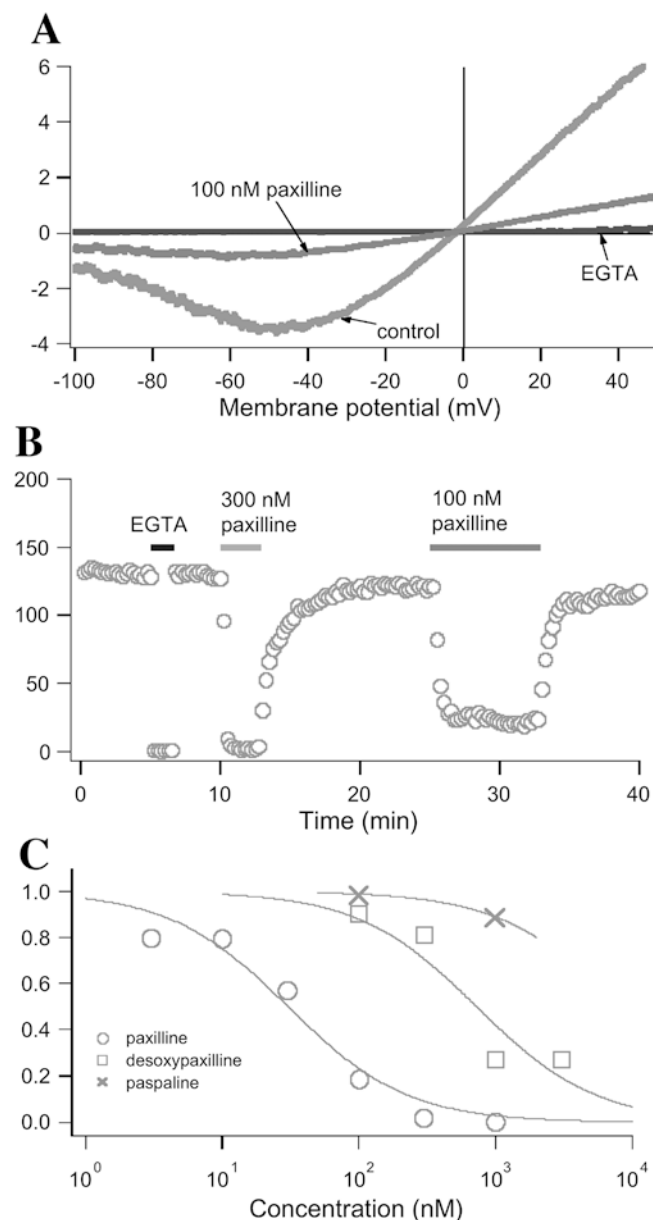


Fig. 7A–C Electrophysiological analysis of maxi-K channel block. **A** Recording of membrane currents from an excised inside-out membrane patch containing about 500 maxi-K channels. The membrane potential was ramped from -100 mV to $+50$ mV over 1 s once every 15 s. **B** Time course of the experiment shown in **A**. Membrane conductance was calculated from the slope of the ramp current between 0 and $+20$ mV, where conductance was maximal. **C** Summary of the concentration-dependence of maxi-K channel blockade by paxilline, desoxypaxilline and paspaline

heterologously expressed maxi-K channels (McManus et al. 1995). The slope conductance measured between 0 and $+20$ mV, where channel activation is maximal, gives a measure of the number of channels available to open, and is plotted over time in Fig. 7B. EGTA rapidly and reversibly reduced the patch conductance to nearly zero, demonstrating that nearly all the current is mediated by maxi-K channels. Paxilline reversibly reduced patch conductance in a concentration-dependent manner.

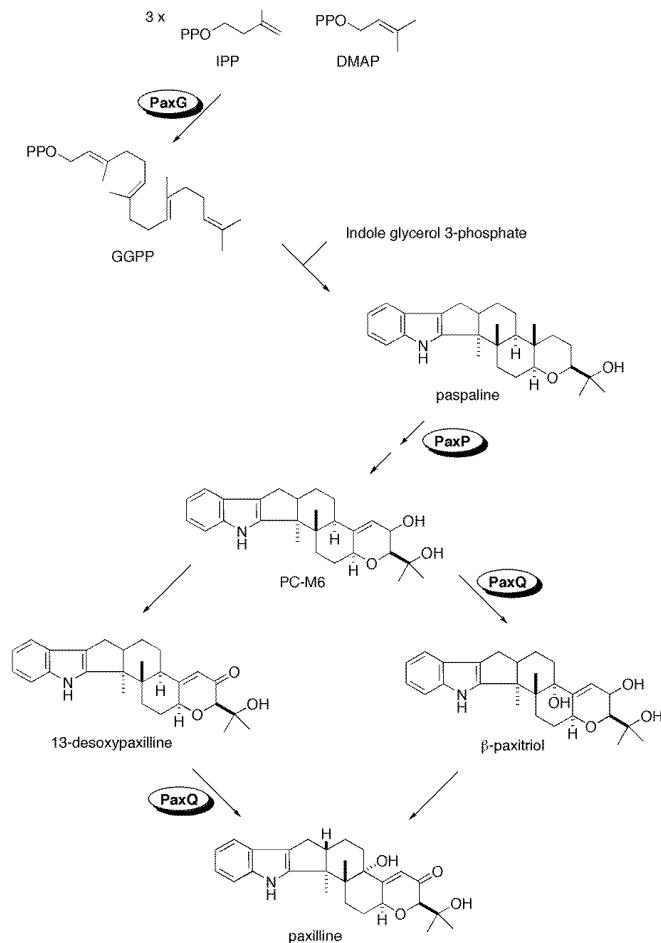


Fig. 8 Proposed pathway for the biosynthesis of paxilline as adapted from Munday-Finch et al. (1996) showing likely steps catalysed by PaxG (geranylgeranyldiphosphate synthase), PaxP (cytochrome P450 monooxygenase) and PaxQ (cytochrome P450 monooxygenase)

Relative reductions in conductance by paxilline, 13-desoxypaxilline and paspaline were calculated in a number of different experiments and are plotted as a function of concentration in Fig. 7C. The data were fitted to Hill equations yielding estimates of K_1 for channel blocking of 30 nM for paxilline, and 730 nM for desoxypaxilline, demonstrating a 24-fold difference in potency between the two compounds. Paspaline was the least effective channel blocker; little blockage was observed at concentrations of up to $1 \mu\text{M}$.

Discussion

The recent cloning of a cluster of genes from *P. paxilli* that are necessary for the biosynthesis of paxilline (Fig. 8) has provided for the first time an insight into the enzymes required for indole-diterpene biosynthesis (Young et al. 2001). The first committed step in the pathway is proposed to be catalysed by PaxG, a GGPP synthase (Fig. 8). The high rates of incorporation of radiolabelled anthranilic acid, compared to tryptophan,

into nodulisporic acid (Byrne et al. 2002) would suggest that indole-3-glycerol phosphate is the primary source of the indole group for this class of compounds (Fig. 8).

The isolation of gene-specific deletion mutants for *paxP* and *paxQ* that accumulate paspaline and 13-desoxypaxilline, respectively, confirms that these genes are essential for paxilline biosynthesis, and that the indole-diterpenes that accumulate are the most likely substrates for the corresponding enzymes, PaxP and PaxQ (Fig. 8). Chemical complementation of *paxG* and *paxP* mutants, but not *paxQ*, for paxilline biosynthesis, by exogenous addition of 13-desoxypaxilline, confirms that these enzymes participate in a common biosynthetic pathway, and that PaxG and PaxP catalyse steps in the pathway that precede that catalysed by PaxQ. However, identification of the products of these reactions will require demonstration in vitro that the purified expressed proteins can catalyse the steps shown in Fig. 8.

Given that a single cytochrome P450 enzyme is required to oxidatively demethylate the 14 position of lanosterol during ergosterol biosynthesis (Trzaskos et al. 1986; Fischer et al. 1989), it is possible that PaxP alone may catalyse the conversion of paspaline to PC-M6 via paspaline B. This hypothesis is supported by recent evidence showing that P450 enzymes required for gibberellin biosynthesis in *Arabidopsis thaliana* (Helliwell et al. 2001) and in *Fusarium fujikuroi* (Rojas et al. 2001) are capable of multiple catalytic steps. Thus, fewer genes/enzymes may be required for paxilline biosynthesis than originally proposed (Young et al. 2001). The metabolic grid proposed by Munday-Finch et al. (1996) suggests that the penultimate substrate for the formation of paxilline could be either 13-desoxypaxilline or β -paxitriol. If this is correct, then PC-M6 may also be a substrate for PaxQ, as the conversion from PC-M6 to β -paxitriol also involves a C-13 hydroxylation. Similarly, the conversion of β -paxitriol to paxilline and of PC-M6 to 13-desoxypaxilline both involve oxygenation at position C-10, suggesting that a single dehydrogenase enzyme may catalyse both reactions. A further prediction from this scheme is that double mutants for *paxQ* and the dehydrogenase gene will accumulate PC-M6.

Comparison of available 3D structures has shown that, although cytochrome P450 enzymes can share as little as 12% sequence identity, all have an enzyme fold that is highly preserved from bacteria to mammals. The alignment of PaxP and PaxQ with four closely related fungal P450s and with two P450s with known 3-D structure has highlighted regions important for substrate binding, redox partner interaction and membrane attachment. The substrate recognition sites (SRS) proposed by Gotoh (1992), and modelled for progesterone binding to 2CS (Williams et al. 2000) (Fig. 2) are only weakly conserved at the amino acid level, even in PaxP and PaxQ, which have similar substrates. These residues for 2C5, circled in blue in Fig. 2, tend to be hydrophobic, a property consistent with the generally hydrophobic nature of P450 substrates. Two residues in the centre of helix I and close to the haem group, Glu267 and

Thr268, have been shown to be important for proton transfer to the haem group during catalysis in BM-3 (Yeom et al. 1995). Aspartic acid often substitutes for Glu267, conserving the carboxylate group, while all of the aligned fungal sequences contain a histidine at this position. The F-G loop has been implicated as one of the membrane-interacting regions of the enzyme (Williams et al. 2000; Murtazina et al. 2002). The 2C5 sequence exhibits an extended F-G loop of 21 residues that contains few charged side chains, which is consistent with the loop's predicted membrane association. In agreement with a cytosolic location, the bacterial BM-3 contains a short F-G loop of just six residues, three of which are potentially charged. The aligned fungal enzymes are generally predicted to have an F-G loop of intermediate length with a mostly hydrophobic character. PaxQ appears to have a much shorter F-G loop of seven residues, while PaxP encodes a loop of 14 residues with seven conserved residues of a hydrophobic nature. The hydrophobicity of other regions (helix A- β -1 and a region preceding helix A), also implicated in membrane interactions for 2C5, is not so well conserved in fungal enzymes. A recent study of the mitochondrial P450 CYP27A by Murtazina et al. (2002) revealed that ten residues in the F-G loop region had important roles in membrane interaction and/or catalytic activity. Sequence similarity between the F-G loops of CYP27A, PaxP and PaxQ identifies six residues that could be important for enzyme function. In particular, two residues (boxed in blue in Fig. 2), located one and four positions, respectively, downstream of the conserved proline have tight constraints on side-chain size and charge to maintain enzyme activity. PaxP and PaxQ contain quite different residues at these two positions, and would be ideal targets for mutagenesis studies. Regions of BM-3 involved in the binding of cytochrome P450 reductase include helices C, L, the meander region and the haem-binding domain. The individual amino acid contacts associated with these protein-protein interactions are circled in red in Fig. 2. The fungal enzymes show a high degree of sequence conservation in these regions, with several amino acids being conserved, in particular an arginine on helix L.

The high levels of paspaline and 13-desoxypaxilline that accumulate in *paxP* and *paxQ* mutants, respectively, have allowed us to purify both compounds and examine their biological activity on high conductance mammalian Ca^{2+} -activated K^{+} (maxi-K) channels. Previous work showed that tremorgenic diterpenes can be divided into two groups, those that inhibit binding of [^{125}I]charybdotoxin (ChTX) to mammalian maxi-K channels, such as aflatrem and penitrem A, and those, such as paxilline and verruculogen, that enhance [^{125}I]ChTX binding (Knaus et al. 1994). Despite these differences both groups of compounds potently inhibited maxi-K channels in electrophysiological experiments (Knaus et al. 1994). By contrast 13-desoxypaxilline had only a marginal effect, with less than 50% inhibition at 30 μM , on maxi-K channels compared to paxilline and verruculogen, which

gave complete inhibition at 1 μ M and 100 nM, respectively. These results indicate that the C-13 OH group on paxilline is important for the biological activity of this tremorgenic mycotoxin. Paspaline, by contrast, is essentially inactive as a channel blocker, causing only slight inhibition at concentrations up to 1 μ M.

The generation of deletion mutants for *paxP* and *paxQ*, which accumulate paspaline and 13-desoxypaxilline, respectively, now opens the way for further biochemical analysis of the enzymatic function of these two cytochrome P450s. A combination of in vivo chemical complementation and in vitro enzymatic assays should resolve the identity of the substrates and products of the reactions catalysed by these enzymes. We also demonstrate here the potential for bioengineering indole-diterpenes with the overproduction in these strains of compounds that can then be used for pharmacological studies. As additional indole-diterpene gene clusters are cloned we will be able to explore the possibility of transferring genes from one organism to another, as has been done for polyketide and non-ribosomal peptide secondary metabolites (Cane et al. 1998), to generate new bioactive molecules.

Acknowledgements This research was supported by grants MAU501 and MAU804 from the New Zealand Foundation for Research, Science and Technology, and a grant (MAU010) from the Royal Society of New Zealand Marsden Fund.

References

- Acklin W, Weibel F, Arigoni D (1977) Zur Biosynthese von Paspalin und verwandten Metaboliten aus *Claviceps paspali*. *Chimia* 31:63
- Al-Samarrai TH, Schmid J (2000) A simple method for extraction of fungal genomic DNA. *Lett Appl Microbiol* 30:53–56
- Altschul SF, Gish W, Miller W, Myers EW, Lipman DJ (1990) Basic local alignment search tool. *J Mol Biol* 215:403–410
- Altschul SF, Madden TL, Schaffer AA, Zhang J, Zhang Z, Miller W, Lipman DJ (1997) Gapped BLAST and PSI-BLAST: a new generation of protein database search programs. *Nucleic Acids Res* 25:3389–3402
- Bairoch A, Bucher P, Hofmann K (1997) The PROSITE database: its status in 1997. *Nucleic Acids Res* 25:217–221
- Belofsky GN, Gloer JB, Wicklow DT, Dowd PF (1995) Antiinsectan alkaloids: shearinines A–C and a new paxilline derivative from the ascostromata of *Eupenicillium shearii*. *Tetrahedron* 51:3959–3968
- Bullock WO, Fernandez JM, Short JM (1987) XL1-Blue: a high efficiency plasmid transforming *recA Escherichia coli* strain with β -galactosidase selection. *Biotechniques* 5:376–378
- Byrd AD, Schardl CL, Songlin PJ, Mogen KL, Siegel MR (1990) The β -tubulin gene of *Epichloë typhina* from perennial ryegrass (*Lolium perenne*). *Curr Genet* 18:347–354
- Byrne KM, Smith SK, Ondeyka JG (2002) Biosynthesis of nodulisporic acid A: precursor studies. *J Chem Soc Chem Commun* 124:7055–7060
- Cane DE, Walsh CT, Khosla C (1998) Harnessing the biosynthetic code: combinations, permutations, and mutations. *Science* 282:63–68
- Cole RJ, Kirksey JW, Wells JM (1974) A new tremorgenic metabolite from *Penicillium paxilli*. *Can J Microbiol* 20:1159–1162
- Cosme J, Johnson EF (2000) Engineering microsomal cytochrome P450 2C5 to be a soluble, monomeric enzyme. Mutations that alter aggregation, phospholipid dependence of catalysis, and membrane binding. *J Biol Chem* 275:2545–2553
- De Jesus AE, Gorst-Allman CP, Steyn PS, van Heerden FR, Vleggar R, Wessels PL, Hull WE (1983) Tremorgenic mycotoxins from *Penicillium crustosum*. Biosynthesis of Penitrem A. *J Chem Soc Perkin Trans I* 1863–1868
- Degtyarenko KN (1995) Structural domains of P450-containing monooxygenase systems. *Protein Eng* 8:737–747
- Deirdre A, Scadden J, Smith CWJ (1995) Interactions between the terminal bases of mammalian introns are retained in inosine-containing mRNAs. *EMBO J* 14:3236–3246
- Engelman DM, Steitz TA, Goldman A (1986) Identifying nonpolar transbilayer helices in amino acid sequences of membrane proteins. *Annu Rev Biophys Biophys Chem* 15:321–353
- Ferreira AVB, Glass NL (1995) PCR from fungal spores after microwave treatment. *Fungal Genet News* 25–26
- Fischer RT, Stam SH, Johnson PR, Ko SS, Magolda RL, Gaylor JL, Trzaskos JM (1989) Mechanistic studies of lanosterol 14 α -methyl demethylase: substrate requirements for the component reactions catalysed by a single P-450 isozyme. *J Lipid Res* 30:1621–1632
- Frohman MA, Dush MK, Martin GR (1988) Rapid production of full-length cDNAs from rare transcripts: amplification using a single gene-specific oligonucleotide primer. *Proc Natl Acad Sci USA* 85:8998–9002
- Garnier J, Gibrat J-F, Robson B (1996) GOR method for predicting protein secondary structure from amino acid sequence. *Meth Enzymol* 266:540–553
- Gatenby WA, Munday-Finch SC, Wilkins AL, Miles CO (1999) Terpendole M, a novel indole-diterpenoid isolated from *Lolium perenne* infected with the endophytic fungus *Neotyphodium lolii*. *J Agric Food Chem* 47:1092–1097
- Giangiaco KM, Fremont V, Mullmann TJ, Hanner M, Cox RH, Garcia ML (2000) Interaction of charybdotoxin S10A with single maxi-K channels: kinetics of blockage depend on the presence of the b1 subunit. *Biochemistry* 39:6115–6122
- Gotoh O (1992) Substrate recognition sites in cytochrome P450 family 2 (CYP2) proteins inferred from comparative analyses of amino acid and coding nucleotide sequences. *J Biol Chem* 267:83–90
- Graham-Lorence SE, Peterson JA (1996) Structural alignments of P450 s and extrapolations to the unknown. *Methods Enzymol* 272:315–326
- Gribskov M, Burgess RR, Devereux J (1986) PEPLOT, a protein secondary structure analysis program for the UWGCG sequence analysis software package. *Nucleic Acids Res* 14:327–334
- Guex N, Diemand A, Peitsch MC, Schwede T (2002) SwissPDB Viewer. <http://www.expasy.ch/spdbv/>
- Gurr SJ, Unkles SE, Kinghorn JR (1987) The structure and organization of nuclear genes of filamentous fungi. In: Kinghorn JR (ed) *Gene structure in eukaryotic microbes*. IRL Press, London, pp 93–139
- Hamill OP, Marty A, Neher E, Sakman B, Sigworth FJ (1981) Improved patch clamp techniques for high resolution current recording from cells and cell-free membrane patches. *Pflugers Archiv* 391:85–100
- Hanner M, Schmalhofer WA, Munujos P, Knaus H-G, Kaczorowski GJ, Garcia ML (1997) The β -subunit of the high-conductance calcium-activated potassium channel contributes to the high-affinity receptor for charybdotoxin. *Proc Nat Acad Sci USA* 94:2853–2858
- Helliwell CA, Chandler PM, Poole A, Dennis ES, Peacock WJ (2001) The CYP88A cytochrome P450, *ent*-kaurenoic acid oxidase, catalyzes three steps of the gibberellin biosynthesis pathway. *Proc Natl Acad Sci USA* 98:2065–2070
- Higgins D, Thompson JN, Gibson TJ, Thompson JD, Higgins DG, Gibson TJ (1994) CLUSTAL W: improving the sensitivity of progressive multiple sequence alignment through sequence weighting, position-specific gap penalties and weight matrix choice. *Nucleic Acids Res* 22:4673–4680

- Huang X-H, Tomoda H, Nishida H, Masuma R, Omura S (1995) Terpendoles, novel ACAT inhibitors produced by *Albophoma yamanashiensis*. I. Production, isolation and biological properties. *J Antibiotics* 48:1–4
- Ichinose H, Wariishi H, Tanaka H (2002) Identification and characterization of novel cytochrome P450 genes from the white-rot basidiomycete, *Coriolus versicolor*. *Appl Microbiol Biotechnol* 58:97–105
- Itoh Y, Johnson R, Scott B (1994) Integrative transformation of the mycotoxin-producing fungus, *Penicillium paxilli*. *Curr Genet* 25:508–513
- Jones DT (1999a) GenTHREADER: an efficient and reliable protein fold recognition method for genomic sequences. *J Mol Biol* 287:797–815
- Jones DT (1999b) Protein secondary structure prediction based on position-specific scoring matrices. *J Mol Biol* 292:195–202
- Knaus H-G, McManus OB, Lee SH, Schmalhofer WA, Garcia-Calvo M, Helms LMH, Sanchez M, Giangiacomo K, Reuben JP, Smith AB, Kaczorowski GJ, Garcia ML (1994) Tremorgenic indole alkaloids potentially inhibit smooth muscle high-conductance calcium-activated channels. *Biochemistry* 33:5819–5828
- Kyte J, Doolittle RF (1982) A simple method for displaying the hydropathic character of a protein. *J Mol Biol* 157:105–132
- Laakso JA, Gloer JB, Wicklow DT, Dowd PF (1992) Sulpinines A-C and secopenitrem B: new antiinsectan metabolites from the sclerotia of *Aspergillus sulphureus*. *J Org Chem* 57:2066–2071
- Laws I, Mantle PG (1989) Experimental constraints in the study of the biosynthesis of indole alkaloids in fungi. *J Gen Microbiol* 135:2679–2692
- Li C, Gloer JB, Wicklow DT, Dowd PF (2002) Thiersinines A and B: novel antiinsectan indole diterpenoids from a new fungiculous *Penicillium* species (NRRL 28147). *Org Lett* 4:3095–3098
- Mantle PG, Weedon CM (1994) Biosynthesis and transformation of tremorgenic indole-diterpenoids by *Penicillium paxilli* and *Acremonium lolii*. *Phytochemistry* 36:1209–1217
- McGuffin LJ, Bryson K, Jones DT (2000) The PSPRED protein structure prediction server. *Bioinformatics* 16:404–405
- McManus OB, Helms LMH, Pallanck L, Ganetzky B, Swanson R, Leonard RJ (1995) Functional role of the β -subunit of high-conductance calcium-activated potassium channels. *Neuron* 14:645–650
- Mende K, Homann V, Tudzynski B (1997) The geranylgeranyl diphosphate synthase gene of *Gibberella fujikuroi*: isolation and expression. *Mol Gen Genet* 255:96–105
- Mount SM (1982) A catalogue of splice junction sequences. *Nucleic Acids Res* 10:459–472
- Munday-Finch SC, Wilkins AL, Miles CO (1996) Isolation of paspaline B, an indole-diterpenoid from *Penicillium paxilli*. *Phytochemistry* 41:327–332
- Murtazina D, Puchkaev AV, Schein CH, Oezguen N, Braun W, Nanavati A, Pikuleva IA (2002) Membrane-protein interactions contribute to efficient 27-hydroxylation of cholesterol by mitochondrial cytochrome P450 27A1. *J Biol Chem* 277:37582–37589
- O'Donnell K, Cigelnik E, Nirenberg HI (1998) Molecular systematics and phylogeography of the *Gibberella fujikuroi* species complex. *Mycologia* 90:465–493
- Ondeyka JG, Helms GL, Hensens OD, Goetz MA, Zink DL, Tsipouras A, Shoop WL, Slayton L, Dombrowski AW, Polishook JD, Ostlind DA, Tsou NN, Ball RG, Singh SB (1997) Nodulisporic acid A, a novel and potent insecticide from a *Nodulisporium* sp. isolation, structure determination and chemical transformations. *J Chem Soc Chem Commun* 119:8809–8816
- Parker R, Siliciano PG (1993) Evidence for an essential non-Watson-Crick interaction between the first and last nucleotides of a nuclear pre-mRNA intron. *Nature* 361:660–662
- Pearson WR, Lipman DJ (1988) Improved tools for biological sequence comparison. *Proc Natl Acad Sci USA* 85:2444–2448
- Pendurthi UR, Lamb JG, Nguyen N, Johnson EF, Tukey RH (1990) Characterization of the *CYP2C5* gene in 21L III/J rabbits. Allelic variation affects the expression of P450IIC5. *J Biol Chem* 265:14662–14668
- Rojas MC, Hedden P, Gaskin P, Tudzynski B (2001) The *P450-1* gene of *Gibberella fujikuroi* encodes a multifunctional enzyme in gibberellin biosynthesis. *Proc Natl Acad Sci USA* 98:5838–5843
- Sambrook J, Fritsch EF, Maniatis T (1989) *Molecular cloning: a laboratory manual* (2nd edn). Cold Spring Harbor Laboratory Press, Cold Spring Harbor, N.Y.
- Sanger F, Nicklen S, Coulson AR (1977) DNA sequencing with chain-terminating inhibitors. *Proc Natl Acad Sci USA* 74:5463–5467
- Sevrioukova IF, Li H, Zhang H, Peterson JA, Poulos TL (1999) Structure of a cytochrome P450-redox partner electron-transfer complex. *Proc Natl Acad Sci USA* 96:1863–1868
- Southern EM (1975) Detection of specific sequences among DNA fragments separated by gel electrophoresis. *J Mol Biol* 98:503–517
- Steyn PS, Vlegaar R (1985) Tremorgenic mycotoxins. *Prog Chem Organic Natural Products* 48:1–80
- Tomoda H, Tabata N, Yang D, Takayanagi H, Omura S (1995) Terpendoles, novel ACAT inhibitors produced by *Albophoma yamanashiensis*. III. Production, isolation and structure elucidation of new components. *J Antibiotics* 48:793–804
- Trzaskos J, Kawata S, Gaylor JL (1986) Microsomal enzymes of cholesterol biosynthesis. Purification of lanosterol 14 α -methyl demethylase cytochrome P-450 from hepatic microsomes. *J Biol Chem* 261:14651–14657
- Tudzynski B, Hölter K (1998) Gibberellin biosynthetic pathway in *Gibberella fujikuroi*: evidence for a gene cluster. *Fungal Genet Biol* 25:157–170
- Tudzynski B, Hedden P, Carrera E, Gaskin P (2001) The P450-4 gene of *Gibberella fujikuroi* encodes ent-kaurene oxidase in the gibberellin biosynthesis pathway. *Appl Environ Microbiol* 67:3514–3522
- Uebele VN, Lagrutta A, Wade T, Figueroa DJ, Liu Y, McKenna E, Austin CP, Bennett PB, Swanson R (2000) Cloning and functional expression of two families of β -subunits of the large conductance calcium-activated K^+ channel. *J Biol Chem* 275:23211–23218
- Unkles SE (1992) Gene organisation in industrial filamentous fungi. In: Kinghorn JR, Turner G (eds) *Applied molecular genetics of filamentous fungi*. Blackie, London, pp 28–53
- Vieira J, Messing J (1987) Production of single-stranded plasmid DNA. *Methods Enzymol* 153:3–11
- Vollmer SJ, Yanofsky C (1986) Efficient cloning of genes of *Neurospora crassa*. *Proc Natl Acad Sci USA* 83:4869–4873
- Weedon CM, Mantle PG (1987) Paxilline biosynthesis by *Acremonium loliae*; a step towards defining the origin of lolitrem neurotoxins. *Phytochemistry* 26:969–971
- Williams PA, Cosme J, Sridhar V, Johnson EF, McRee DE (2000) Mammalian microsomal cytochrome P450 monooxygenase: structural adaptations for membrane binding and functional diversity. *Mol Cell* 5:121–131
- Yeom H, Sligar SG, Li H, Poulos TL, Fulco AJ (1995) The role of Thr268 in oxygen activation of cytochrome P450BM-3. *Biochemistry* 34:14733–14740
- Yoder OC (1988) *Cochliobolus heterostrophus*, cause of southern corn leaf blight. *Adv Plant Pathol* 6:93–112
- Young C, Itoh Y, Johnson R, Garthwaite I, Miles CO, Munday-Finch SC, Scott B (1998) Paxilline-negative mutants of *Penicillium paxilli* generated by heterologous and homologous plasmid integration. *Curr Genet* 33:368–377
- Young CA, McMillan L, Telfer E, Scott B (2001) Molecular cloning and genetic analysis of an indole-diterpene gene cluster from *Penicillium paxilli*. *Mol Microbiol* 39:754–764